The Exchange-Correlation Effects on the Electronic Bands of Hybrid Armchair Single-Walled Carbon Boron Nitride Nanostructure

Yahaya Saadu Itas [1], Abdussalam Balarabe Suleiman [2], Chifu E. Ndikilar [2], Abdullahi Lawal [3], Razif Razali [4], Mayeen Uddin Khandaker [5,*], Pervaiz Ahmad [6], Nissren Tamam [7] and Abdelmoneim Sulieman [8]

[1] Department of Physics, Bauchi State University Gadau, PMB 65, Gadau 751105, Nigeria; yitas@basug.edu.ng
[2] Department of Physics, Federal University Dutse, Dutse 720101, Nigeria; salam@fud.edu.ng (A.B.S.); chifu.ndikilar@fud.edu.ng (C.E.N.)
[3] Department of Physics, Federal College of Education, Zaria 810282, Nigeria; labdullahi2@live.utm.my
[4] Department of Physics, Faculty of Science, Universiti Teknologi Malaysia, Skudai 81310, Malaysia; razifrazali@utm.my
[5] Centre for Applied Physics and Radiation Technologies, School of Engineering and Technology, Sunway University, Bandar Sunway 47500, Malaysia
[6] Department of Physics, University of Azad Jammu and Kashmir, Muzaffarabad 13100, Pakistan; pervaiz.ahmad@ajku.edu.pk
[7] Department of Physics, College of Sciences, Princess Nourah bint Abdulrahman University, P.O. Box 84428, Riyadh 11671, Saudi Arabia; nmtamam@pnu.edu.sa
[8] Department of Radiology and Medical Imaging, College of Applied Medical Sciences, Prince Sattam Bin Abdulaziz University, P.O. Box 422, Alkharj 11942, Saudi Arabia; a.sulieman@psau.edu.sa
* Correspondence: mayeenk@sunway.edu.my

Abstract: This study investigates the effect of exchange-correlation on the electronic properties of hybridized hetero-structured nanomaterials, called single-walled carbon boron nitride nanotubes (SWCBNNT). A first principles (ab initio) method implemented in Quantum ESPRESSO codes, together with different parametrizations (local density approximation (LDA) formulated by Perdew Zunga (PZ) and the generalized gradient approximation (GGA) proposed by Perdew–Burke–Ernzerhof (PBE) and Perdew–Wang 91 (PW91)), were used in this study. It has been observed that the disappearance of interface states in the band gap was due to the discontinuity of the π–π bonds in some segments of SWCNT, which resulted in the asymmetric distribution in the two segments. This work has successfully created a band gap in SWCBNNT, where the PBE exchange-correlation functional provides a well-agreed band gap value of 1.8713 eV. Effects of orbitals on electronic properties have also been studied elaborately. It has been identified that the P^y orbital gives the largest contribution to the electrical properties of our new hybrid SWCBNNT nanostructures. This study may open a new avenue for tailoring bandgap in the hybrid heterostructured nanomaterials towards practical applications with next-generation optoelectronic devices, especially in LED nanoscience and nanotechnology.

Keywords: SWCBNNT heterostructures; hybrid system; quantum ESPRESSO; band gap; GGA functionals

1. Introduction

Carbon nanotubes (CNTs) have been evolved as important materials for the advancement of nanoscience and technology [1]. They have received much attention because of their ability to behave as both metallic and semi-metals depending on the chirality/translation of carbon atoms arranged in a hexagonal lattice [2]; they can be single-walled (SW) or multi-walled (MW) structures. They are anisotropic and also exist in three different geometries as an armchair, zigzag, and chiral. To bring the CNTs to the next-generation optoelectronic fields or applications, many research approaches comprising theoretical [3], computational, and experimental [4] ideas are carried out, and they all come up with many exciting results [5,6]. A wide range of potential applications of CNTs in the field of polymer,

composites, hydrogen/energy storage, biomedical sciences, field emission dipoles, etc., were also reported. Although CNTs show unique structural and physical properties, they still require further improvement to be used in certain fields of nanotechnology [7]. As a result, CNTs hetero-structures have become one of the most interesting areas where scientists are trying to explore novel properties for application purposes. The CNT composites such as carbon nanotube metal matrix composites (CNT-MMC) are formed to make alloys due to the CNT's high tensile strength and electrical conductivity. Copper/carbon nanocomposites are produced to fill the high demand for copper substitutes [8]. CNT composites are used as reinforcement and thermal reservoirs. The high demand for semiconductor devices today has led us to develop the idea of combining SWCNT with a wide gap material such as boron nitride nanotube (BNNT) to form a CNT–BNNT hetero-structure. The hybrid single-walled carbon boron nitride nanotube (SWBNNT) has an identical hexagonal structure to that of a single-walled carbon nitride nanotube (SWCNT). It is worth mentioning that a single-walled boron nitride nanotube (SWBNNT) is an insulator or wide bandgap semiconductor with an energy gap of 5–6 eV [9], whereas armchair SWCNT is a conductor in its pure form [10]. Therefore, the idea of creating a carbon boron nitride nanotube heterostructure may create an energy band gap in CNT which will reduce its electrical conductivity to the level of semiconductors. Just like CNTs, the BNNT is thermally and chemically inert, and is known for its anisotropic behavior [11]. It is an isomorph of graphene [12]. Generally, armchair SWCNTs are rarely used as pure semiconductors because of compatibility problems that arose from their hexagonal structure and isotropic nature [13]. SWCNTs are used as semiconductors when they are fabricated in an impure form, where the intrinsic impurities result in the creation of a band gap that reduces and/or tries to terminate the full electrical behavior of the nanotubes. Successful creation of CBNNT hybrid nanotubes can only be achieved when we use a nanotube of the same structural properties, such as crystallographic nature (hexagonal structure), anisotropy, piezoelectricity, pyroelectricity, and biocompatibility. A successful attempt was made to create a band gap in CNT with the optimized structure of bilayered tin selenide (SnSe) [14] by using the Quantum ESPRESSO package. Tin selenide (SnSe) has a hexagonal honeycomb structure similar to graphene with a separation of 1.56 Å between Sn and Se atoms [14–16]. The result was the creation of a SnSe-CNT semiconductor with a narrow bandgap of 2.56 eV. The Perdew–Burke–Ernzerhof (PBE) type of generalized gradient approximation (GGA) exchange-correlation was used to obtain the said result. Following the same strategy, as demonstrated in the literature [17], we have been motivated to study the electronic band structures for hybrid SWCBNNT structures. Consequently, in this work, we have implemented the ab initio principles to calculate the electronic properties of our newly created system of carbon boron nitride nanotubes (CBNNT) and analyze its potential in the next generation semiconductor applications. Some of the relevant works on the effect of exchange correlations and band gaps obtained both theoretically and experimentally are summarized in Table 1.

Table 1. Available studies on band gap in hybrid nanostructures by various methods.

DFT Method	Theoretical Results	Experimental Results	References
DFT-theoretical	Reported the possibility of obtaining band gap by combining CNT segments and BNNT segments.	None	[18]
DFT-Theoretical	It has been reported that the CNT-BNNT can be competitive in thermodynamical stability for sufficiently large segments of building blocks in the axial direction.		[19]
Non-equilibrium Green's function method combined with the density functional theory	Carbon and boron nitride nanotubes were obtained with semiconducting properties of 2.2 eV; results predicted that CBNNT could become potential candidates in the field of nano rectifiers.		[20]

Table 1. *Cont.*

DFT Method	Theoretical Results	Experimental Results	References
Density functional theory and using basis set 6–31 g (d,p)	Reported the band gap of 1.21 and 2.52 eV which is close with our results of PW91.		[21]
Geometry optimization implemented in the CASTEP package	Reported 2.3 eV band gap in hetero nanotubes with the lowest unoccupied molecular orbital and the highest occupied molecular orbital mainly located on the carbon nanotube section.		[22]
Vienna ab initio simulation package	The electrical conductivity of CBNNT is increased by oxygen absorption.		[23]
CVD		2.41 eV band gap was reported. Recommended for theoretical and computational confirmatory tests.	[24]
VASP code	Reported 1.06 eV band gap, also reported that the highest occupied and lowest unoccupied orbital gap of carbon-boron-nitride hetero nanotubes can be significantly tuned by modifying the CNT and BNNT general geometry.		[25]
LDA	Reported 5.6 eV band gap in BNNT. Furthermore, analysis of the HOMO–LUMO gap after the adsorption process showed that the HOMO value increased marginally while the LUMO value decreased dramatically in the curcumin-BNNT complexes		[26]
GGA-PBE	Reported 1.83 eV band gap, which agrees with this current research. Also, reported that the band gap of the CBNNT system is greatly influenced by the nanotube aspect ratio.		[27]
GGA-PW91	Reported 2.52 eV band gap, highlighted the potentials of CBNNT for the next generation spintronics.		[28]

As can be seen in Table 1, various methods have been used to study CBNNT nanostructures, and various results have been obtained. In our work, a novel method of inter-tube coupling (which is the basis of this research) was used (Figure 1). As far as our concern, our technique was not adopted in any of the previous studies available in the literature. As such, this work forms a new pathway for tailoring band gap in hybrid heterostructured nanomaterials for advanced optoelectronic applications.
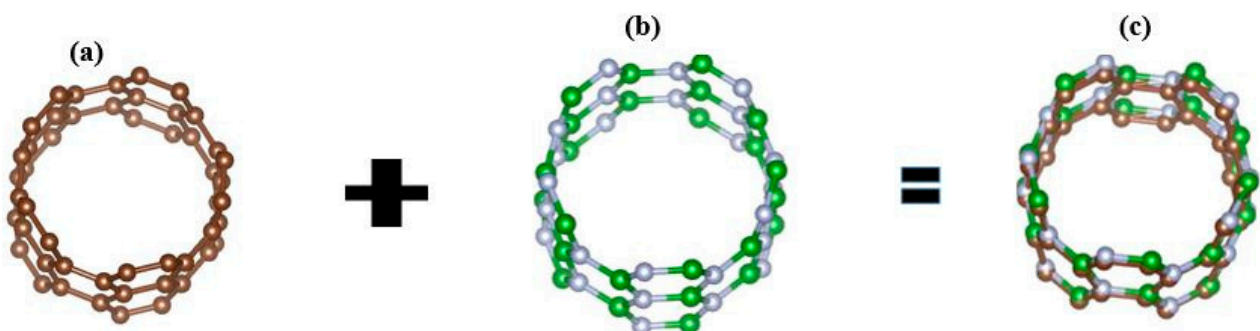

Figure 1. Hybrid SWCBNNT hetero-nanotubes optimized by inter-tube coupling. (**a**) Metallic (5, 5) SWCNT (**b**) Non-metallic (5, 5) SWBNNT and (**c**) Semi-conducting (5, 5) SWCBNNT.

2. Computational Methods

This section demonstrates the adopted working methodology that has made possible the successful implementation of this study. The method shows effectiveness in developing a new set of processes that could eventually help the relevant researchers for creating a new band gap in the potential hetero-combination of BNNT-CNT nanostructures. In this study, a representative model of both (5, 5) armchair SWBNNT and SWCNT was considered. The local density of state (LDOS), the total density of state (DOS), and the electronic band's structure of the armchair form of CBNNT hetero-nanotubes are calculated within the self-consistent field through solving the Kohn–Sham equation within the DFT in terms of LDA and GGA functional (a method implemented on Quantum ESPRESSO codes), this is necessary in order to analyze the effect of the various exchange-correlation functional on the bands' alignment of our hetero-system. The Quantum ESPRESSO (an acronym for open-Source Package for Research in Electronic Structure, Simulation, and Optimization) is an integrated suite of open-source computer codes for electronic-structure calculations and materials modeling at the nanoscale. It is based on density-functional theory, plane waves, and pseudopotentials. It uses first-principles electronic-structure calculations and materials modeling, distributed for free and as free software under the GNU General Public License.

Calculations are performed on the $2 \times 2 \times 1$ supercell model of (5, 5) SWBNNT primitive unit cell containing 80 carbon atoms and 16 atoms each of boron and nitrogen, based on the first principles together with DFT implemented in quantum ESPRESSO codes. The calculations for the exchange-correlation are performed within the Perdew-Zunga (PZ) within LDA, Perdew–Burke–Ernzerhof (PBE), and Perdew–Wang 91 (PW91) of GGA approximations together with the smearing occupations method of integrals. We have determined the Brillouin zone by using the Monkhorst–Pack scheme with k-grids of $1 \times 1 \times 4$ and an e-cut of 50 Ry.

3. Geometry Optimization

Because of the structural influence of the hybrid SWCBNNT system on the electronic properties, optimization of the tube geometry was performed prior to the calculation of the electronic properties. This is achieved with the codes implemented in the nanotubes modeler and VESTA. The hetero-nanotube was optimized by a new method called inter-tube coupling (Figure 1) in which the carbon atoms in CNT are coupled with boron and nitrogen atoms in BNNT.

The studies were conducted on the SWCBNNT system and the inter-tube separations were chosen as 3.95 Å, 4.80 Å, and 5.29 Å respectively. To ensure accurate results in this research, the nanotube was appropriately relaxed to appropriate geometries. In the SWCBNNT, the tube length and the tube height were chosen as 6.23 Å and 4.26 Å, respectively. The chiral/translation vectors were constructed such that $n = 5$, $m = 5$ to ensure the proper armchair chirality. The results of the relax calculations are listed in Table 2. The maximum force, stress, and displacements were set at 0.06 eV/Å, 0.06 GPa, and 6×10^{-4} Å, respectively. The unit cell volume was 6515.67 Å^3 with lattice parameters a = 18.68 Å and c = 9.68 Å. As can be seen from iteration 3, there was zero error in the relax calculations; as such, the data in iteration 3 were used to obtain a well-converged value of all parameters used in this research.

Table 2. The geometry of SWCBNNT (5, 5).

Iterations	Delta-h	Delta-r	K-Point (Gamma)			Iterations		
						a_1	a_2	a_3
0			1.000000	1.000000	1.000000	41	41	0
1	1.7171×10^{-3}	7.5733×10^{-2}	1.001208	1.001208	1.000000	20	20	0
2	-4.1446×10^{-5}	-1.8236×10^{-4}	1.001205	1.001205	1.000000	0	0	0
3	$0.0000e + 00$	$0.0000e + 00$	1.001205	1.001205	1.000000			

4. Results and Discussion

4.1. Bands Structures of (5, 5) CBNNT under Three Different Exchange-Correlation Functionals

The electronic band structures of the system of (5, 5) armchair single-walled carbon boron nitride nanotubes (SWCBNNT) hybrid material were studied, and the results are compared under three different exchange-correlation functional implemented within the local density approximation (LDA) and the generalized gradient approximation (GGA). The results obtained with each pseudopotential showed that direct band gaps [29] were obtained, with LDA-PZ pseudo potential being the lowest of 0.0433 eV at the gamma point. A considerable improvement of the band gap was obtained when PBE pseudopotential was used for our calculations. As can be seen in Figures 2b and 3b, a direct band gap of 1.87 eV was achieved with PBE and 0.1886 with PW91 (as presented in Figures 2c and 3c. The result obtained with PBE is close to the value of 2.00 eV experimental value [30]. This value of band gap makes the CBNNT behave as a semi-metal with a tunable direct band gap [31], a property that can be applied in LED, spintronic, electronic, Schottky devices, and photonics devices with tunable band structures [32].
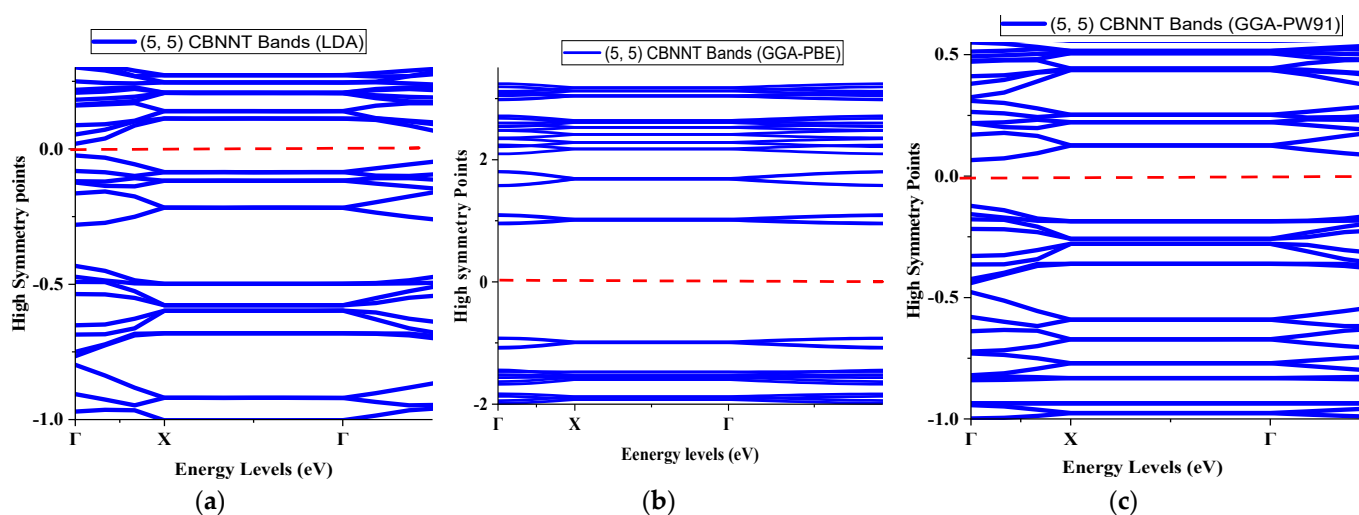

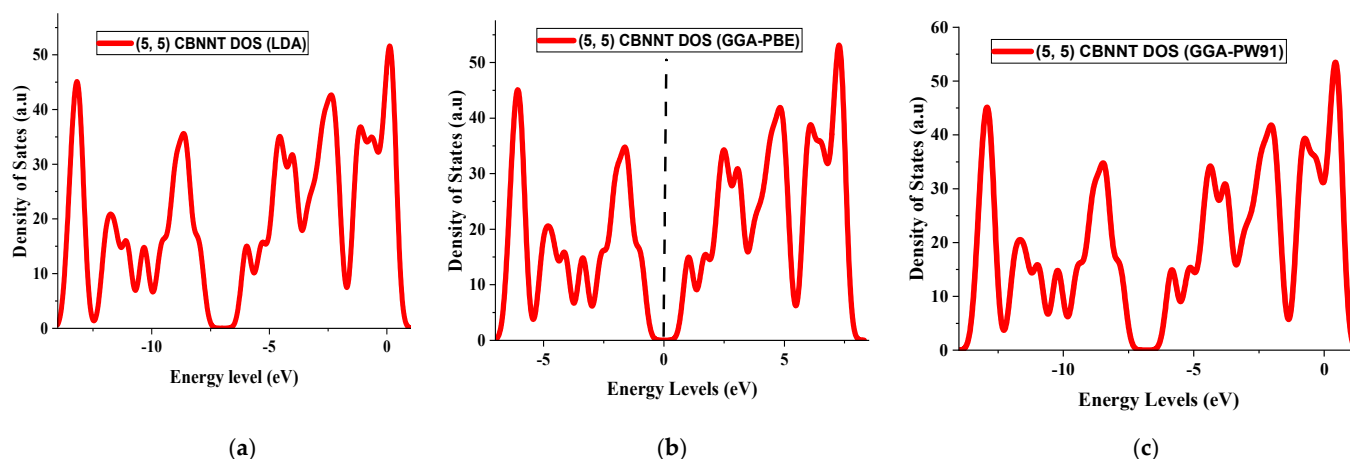**Figure 2.** Bands structures of (5, 5) SWCBNNT (**a**) LDA (**b**) PBE (**c**) PW91.

Figure 3. TDOS for (5, 5) CBNNT systems under three different exchange-correlations of LDA and GGA. (**a**) Effect of LDA; (**b**) effect of PBE; (**c**) effect of PW91.

The effect of each pseudopotential is summarized in Table 3. It can be seen that different total energies were achieved by various exchange-correlation functional; for example, the total energy was −12.99 Ry with PZ functional. This gives a Fermi energy

of −8.16 eV in 72 self-consistent fields (SCF) iterations. However, different total energy and Fermi energy were obtained by PBE functional, although the SCF calculation was achieved in the same 72 iterations. In the case of PW91, the total energy achieved was −1314.24 Ry (i.e., Rydberg unit of energy) and the Fermi energy was −8.00 eV. Since the highest band gap was achieved with PBE exchange functional, we consider it as the optimum parameter of the generalized gradient approximation in solving the exchange-correlation problem, because it is reported in previous studies that the PBE is faster than the other exchange-correlation [33].

Table 3. The effect of exchange-correlation in the Fermi energy.

S/No	Pseudopotential	Total Energy Achieved (Ry)	The Calculated Band Gap (eV)	SCF Iterations
1	LDA	−1299.17	0.043	72
2	PBE	−1444.79	1.87	72
3	PW91	−1314.23	0.19	74

4.2. Analysis of the Density of States

To verify more on the findings regarding the bands obtained, analyses were made on the density of states and partial density of states for our SWCBNNT hybrid system. As can be seen in Figure 3a,b, there are more states in the valence band than in the conduction band for bands obtained with PZ and PW91 exchange functional. This is because the total energy of the nanotube that contributes to the conduction is lower than the sum of the energy which forms the hetero-nanotube. As a result, the total energy of the nanotube which contributes to conduction is lower than the sum of the energy which forms the hetero-nanotube. Direct bands are obtained because the highest energy of the valence band is equal to the lowest energy of the conduction band. It means that they are at the same momentum when the transition takes place [34]. Recombination of holes and electron takes place in order to conserve the momentum energy that is released in the form of light, such as LED. A good band can be seen in Figure 3b when PBE exchange functional was used. Although the PBE underestimates band gaps, this value is close to the 2.0 eV experimental value reported elsewhere [35]. Figure 3b gives the plot information of TDOS for (5, 5) SWCBNNT system within the PBE implementation. Zero states can be seen at the Fermi level; as such, this region can be considered as the gap calculated to be 1.8713 eV. Very few states can be seen in Figure 3a,b. There are also more states in the conduction band than in the valence band. The three highest peaks can be seen with different states. The first one, at −6.109 eV, is due to domination by $1S^2$ orbital of boron and carbon atoms, respectively (refer to Figures 4a,b and 5a,b). The second peak, at −1.709 eV, is due to collective contributions by $2S^2$ orbitals of B, C, and N atoms, respectively [36]. Lower occupations are due to partial contributions by S orbitals of all the systems (refer to Figure 4). The third state occurs at 7.291 eV. This is due to collective dominations by $2P^y$ orbitals of B, C, and N atoms. The presence of zero states at zero energy level confirms that the band gap had been successfully created by using PBE exchange functional. In the case of the PW91 exchange functional, dense states are seen in the valence bands because the total energy of interactions is the sum of exchange energy and interaction energy of the nanotube which contributes to the conduction band, and that is lower than the sum of the formation energy which forms the hetero-nanotube.
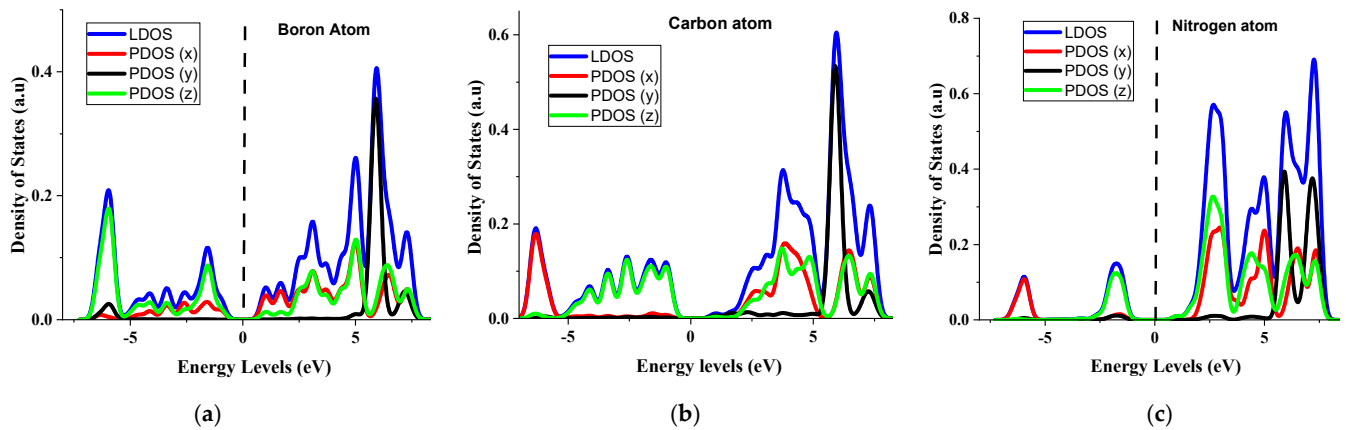
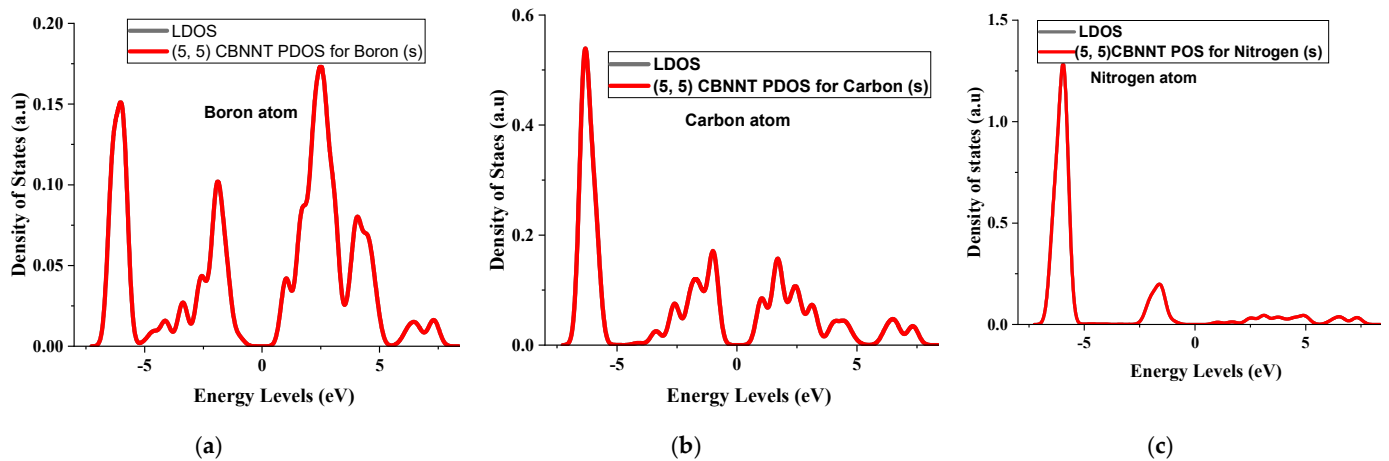**Figure 4.** PDOS of (5, 5) CBNNT system under GGA-PBE. (**a**) Boron atom (**b**) carbon atom (**c**) Nitrogen atom.

Figure 5. S orbital contribution to electrical properties of (5, 5) CBNNT system. (**a**) Boron atom (**b**) carbon atom (**c**) Nitrogen atom.

4.3. Partial Density of States for the (5, 5) CBNNT System

These studies of PDOS are limited to the results implemented with LDA and PBE exchange functional. The individual orbital's contributions and effect on the hybridized SWCBNNT system were studied. The SWCBNNT semiconductor created in this work is only a hybrid of S and P orbitals. Moreover, all the constituent elements belonging to the same group IV in the periodic table with only carbon, among them, can form a covalent bond to itself with electron mobility of 15,000 cm^2/Vs in the graphene lattice [37]. The studies of PDOS therefore may help to understand the electrical mobility of our semiconductor system. Figure 6 shows that P^y orbital generally determines the band gap of our SWCBNNT hybrid system because it gives the largest contribution in all the constituent elements. However, our investigation revealed that P^x orbital provided the smallest contribution to the conduction process. This is because they are considered frozen and form some part of the nucleus. They are also always filled with both up and down spins, hence requiring more energy of excitation [38]. The P^z orbitals are partially occupied with less probability of finding the electron. For example, the P^z orbital of carbon is having zero electrons; hence, will have to make a little contribution by interaction with one of the 2S electrons. The interaction between each P^z orbitals among the carbon atoms is due to the result of the π-bonding. Therefore, the electrical mobility across the Fermi energy is mainly by the carbon atoms in the carbon nanotube lattice. This can be justified from Figure 3, which shows that the P^z orbital of carbon contributes more than the P^z orbitals of boron and nitrogen atoms.
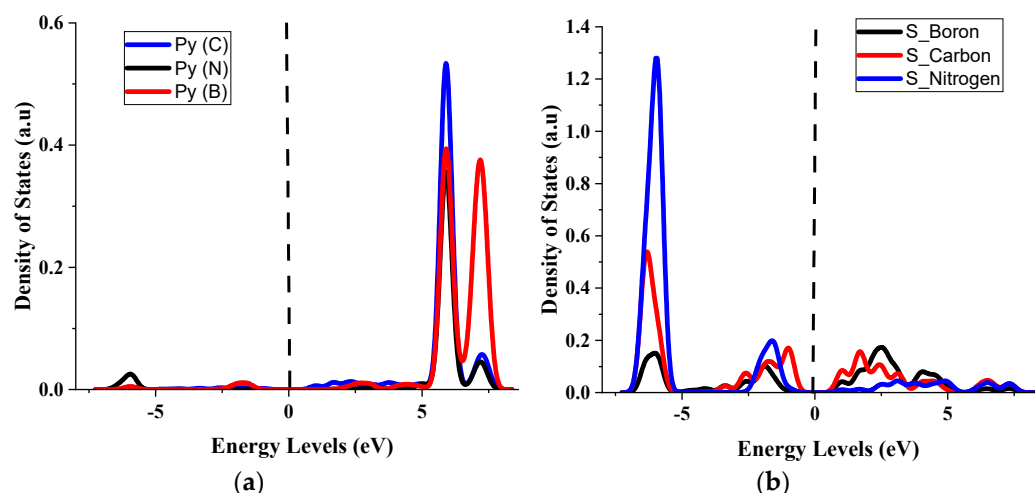
Figure 6. (**a**) P^y contributions for B, C, and N, respectively; (**b**) S contributions for B, C, and N, respectively.

There is a little contribution by the S orbital of carbon because of its interaction with carbon P^z orbitals. The S orbitals of other elements can be seen to make almost no contributions. To justify this claim, the PDOS and LDOS of Figure 5 can be seen to overlap, which means that the local density of states is the contribution of the S orbital.

4.4. Effects of P^y and S Orbitals in the Semiconductivity of (5, 5) CBNNT

To report which of the P^y orbitals takes more of the electronic properties of our system, we analyzed the results shown in Figure 6. This figure reveals that the P^y orbital of carbon in SWCNT provides more dominations than the P^y orbitals of boron and nitrogen in SWBNNT. Therefore, it can be inferred that P^y orbitals of carbon contribute to narrowing the wider gap made by boron nitride nanotubes, which pave the way for semiconductivity. The results of this work agreed closely with previous findings from different methods. For example, ref. [18] reported that it is possible to obtain a new set of semiconducting hetero nanotubes by interfacing layers of CNT and BNNT. This has been possible in this work. The 1.8 eV band gap reported by [27] agrees with the result of 1.8713 eV obtained with the same PBE in this work. Moreover, the reported value of 1.21 by [21] is approximately close to the obtained 0.8 eV in this work with the same PW91.

Figure 6a illustrates the individual p^y contributions by each of the constituent elements, although they all belong to the same group in the periodic table [39]. They differ in the contribution to the conduction process by each of their p-orbitals, which arises due to different occupations by p^z orbital [40]. For example, the p^z orbital for element boron contributes to the electronic configuration $1S^2 2S^2 2P_x^1 2P_y^0 2P_z^0$. As can be seen, the p^y orbital of boron contributes less because it has zero electrons. In the case of carbon with an electronic configuration of $1S^2 2S^2 2P_x^1 2P_y^1 2P_z^0$, it can be seen that the p^y orbital of carbon is occupied by one electron, hence making a higher contribution than boron. This can be seen in Figure 6b. All the S' orbitals (Figure 6b) are found to make a very negligible contribution to the conduction process because they are considered frozen and form some part of the nucleus [41–46]. They are also always filled with both up and down spins, hence requiring more energy of excitation similar to p^x orbital.

5. Conclusions

In this study, the electronic structure of the hybridized armchair form of SWCBNNT was calculated based on the first principles method. This study successfully created a band gap under three different parameterizations of LDA and GGA using the density functional theory which is implemented in Quantum ESPRESSO code. In each case, the armchair configurations of carbon nanotubes and boron nitride nanotubes were chosen to form

coupled carbon–boron–nitride nanotubes via a new method of inter-tube coupling. The chirality of all systems was chosen to be that of (5, 5) armchair tube. It was found that the band structure of our (5, 5) SWCBNNT is straightforward, and can be applied in the next-generation optoelectronic devices such as LED. The band gap of the hybrid SWCBBNNT system is seen to greatly depend on the orbital contributions to atomic interactions in which the p^y orbitals of carbon in SWCNT accounted for the electronic properties of the CBNNT hetero nanotubes material. This is because other p^x and p^z orbitals are considered to form some part of the nucleus which provide effective repulsion; hence, valence states are orthogonal to the core nuclear states and are considered frozen. Although the band gap of 1.8 eV has been recorded with PBE, it is well known that both LDA and GGA underestimate the band gap. This result, therefore, can be improved by using hybrid functions such as the GW functionals. The calculation of these band structures may hopefully lead to the addition of new knowledge in the literature, and then serve as a reference for further research on CBNNT heterostructures.

References

1. Wilson, M.; Evans, L. Carbon Nanotubes as Advanced Materials. *J. Aust. Ceram. Soc.* **2021**, *36*, 21–36.
2. Powell, L.R.; Kim, M.; Wang, Y. Chirality-Selective Functionalization of Semiconducting Carbon Nanotubes with a Reactivity-Switchable Molecule. *J. Am. Chem. Soc.* **2017**, *139*, 12533–12540. [CrossRef] [PubMed]
3. Melaibari, A.; Daikh, A.A.; Basha, M.; Abdalla, A.W.; Othman, R.; Almitani, K.H.; Hamed, M.A.; Abdelrahman, A.; Eltaher, M.A. Free Vibration of FG-CNTRCs Nano-Plates/Shells with Temperature-Dependent Properties. *Material* **2022**, *10*, 583. [CrossRef]
4. Janas, D. Special Issue of Materials Focused on "Electrical, Thermal and Optical Properties of Nanocarbon Materials". *Materials* **2022**, *15*, 1649. [CrossRef] [PubMed]
5. Foygel, M.; Morris, R.D.; Anez, D.; French, S.; Sobolev, V.L. Theoretical and computational studies of carbon nanotube composites and suspensions: Electrical and thermal conductivity. *Phys. Rev. B* **2015**, *71*, 1–6. [CrossRef]
6. Zhigilei, L.V.; Salaway, R.N.; Wittmaack, B.K.; Volkov, A.N. Computational Studies of Thermal Transport Properties of Carbon Nanotube Materials. In *Carbon Nanotubes for Interconnects*; Springer: Cham, Switzerland, 2017; pp. 129–161. [CrossRef]
7. Trivedi, M. Recent Development and Applications of Carbon Nanotubes. *Chem. Sci. Rev. Lett.* **2020**, *9*, 502–510. [CrossRef]
8. Sundaram, R.M.; Sekiguchi, A.; Sekiya, M.; Yamada, T.; Hata, K. Copper/carbon nanotube composites: Research trends and outlook. *R. Soc. Open Sci.* **2018**, *5*, 180814. [CrossRef]
9. Kim, K.S.; Kim, M.J.; Park, C.; Fay, C.C.; Chu, S.-H.; Kingston, C.T.; Simard, B. Scalable manufacturing of boron nitride nanotubes and their assemblies: A review. *Semicond. Sci. Technol.* **2016**, *32*, 3–13. [CrossRef]
10. Saifuddin, N.; Raziah, A.Z.; Junizah, A.R. Carbon Nanotubes: A Review on Structure and Their Interaction with Proteins. *J. Chem.* **2013**, *2013*, 676815. [CrossRef]
11. Yanar, N.; Yang, E.; Park, H.; Son, M.; Choi, H. Boron Nitride Nanotube (BNNT) Membranes for Energy and Environmental Applications. *Membranes* **2020**, *10*, 430. [CrossRef]
12. Nematollahi, P.; Esrafili, M.D.; Bagheri, A. Functionalization of single-walled (n, 0) carbon and boron nitride nanotubes by carbonyl derivatives (n = 5, 6): A DFT Study. *Can. J. Chem.* **2016**, *94*, 2–21. [CrossRef]

13. Gharbavi, K.; Badehian, H. Structural and electronic properties of armchair (7, 7) carbon nanotubes using DFT. *Comput. Mater. Sci.* **2014**, *82*, 159–164. [CrossRef]
14. Itas, Y.S.; Ndikilar, C.E.; Zangina, T.; Hafeez, H.Y.; Safana, A.A.; Khandaker, M.U.; Ahmad, P.; Abdullahi, I.; Olawumi, B.K.; Babaji, M.A.; et al. Synthesis of Thermally Stable h-BN-CNT Hetero-Structures via Microwave Heating of Ethylene under Nickel, Iron, and Silver Catalysts. *Crystal* **2021**, *11*, 1097. [CrossRef]
15. Ahmadi, S.; Raeisi, M.; Eslami, L.; Rajabpour, A. Thermoelectric Characteristics of Two-Dimensional Structures for Three Different Lattice Compounds of B-C-N and Graphene Counterpart BX (X = P, As, and Sb) Systems. *J. Phys. Chem.* **2021**, *125*, 14525–14537. [CrossRef]
16. Shao, J.; Beaufils, C.; Kolmogorov, A.N. Ab initio engineering of materials with stacked hexagonal tin frameworks. *Sci. Rep.* **2016**, *6*, 28369. [CrossRef]
17. Omidvar, A.; Hadipour, N. Density functional theory studies of carbon nanotube-Graphene nanoribbon hybrids. *J. Iran. Chem. Soc.* **2013**, *10*, 1239–1246. [CrossRef]
18. An, W.; Turner, H. Linking Carbon and Boron-Nitride Nanotubes: Heterojunction Energetics and Band Gap Tuning. *J. Phys. Chem. Lett.* **2010**, *1*, 2269–2273. [CrossRef]
19. Kostoglou, N. Boron Nitride Nanotubes Versus Carbon Nanotubes: A Thermal Stability and Oxidation Behavior Study. *Nanomaterials* **2020**, *10*, 2435. [CrossRef]
20. An, Y.; Sun, Y.; Jiao, J.; Zhang, M.; Wang, K.; Chen, X.; Wu, D.; Wang, T.; Fu, Z.; Jiao, Z. The rectifying effect of heterojunctions composed of carbon and boron nitride nanotubes. *Org. Electron.* **2017**, *50*, 43–47. [CrossRef]
21. El-Barbary, A.A.; Eid, K.M.; Kamel, M.A.; Taha, H.O.; Ismail, G.H. Adsorption of CO, CO_2, NO and NO_2 on Carbon Boron Nitride Hetero Junction: DFT Study. *J. Surf. Eng. Mater. Adv. Technol.* **2015**, *5*, 57979. [CrossRef]
22. Hong-Xia, L.; He-Ming, Z.; Jiu-Xu, S.; Zhi-Yong, Z. Electronic transport properties of an (8, 0) carbon/boron nitride nanotube heterojunction. *Chin. Phys. B* **2010**, *19*, 037104. [CrossRef]
23. Liu, H.; Turner, H. Oxygen Adsorption Characteristics on Hybrid Carbon and Boron-Nitride Nanotubes. *Comput. Chem.* **2014**, *35*, 1058–1063. [CrossRef] [PubMed]
24. Yap, Y.K. *Hetero-Junctions of Boron Nitride and Carbon Nanotubes: Synthesis and Characterization*; Technical Report No. DOE-MTU-ER46294; Michigan Technological University: Houghton, MI, USA, 2013; pp. 1–7.
25. Ahmad, P.; Khandaker, M.U.; Khan, Z.R.; Amin, Y.M. Synthesis of boron nitride nanotubes via chemical vapour deposition: A comprehensive review. *RSC Adv.* **2015**, *5*, 35116–35137. [CrossRef]
26. Nafiu, S.; Apalangya, V.A.; Yaya, A.; Sabi, E.B. Boron Nitride Nanotubes for Curcumin Delivery as an Anticancer Drug: A DFT Investigation. *Appl. Phys.* **2022**, *12*, 879. [CrossRef]
27. Liu, H.; Zhang, H.; Song, J.; Zhang, Z. Electronic structures of an (8, 0) boron nitride/carbon nanotube heterojunction. *J. Semicond.* **2010**, *31*, 013001. [CrossRef]
28. Dhungana, K.; Pati, R. Boron nitride nanotubes for spintronics. *Sensors* **2014**, *14*, 17655–17685. [CrossRef] [PubMed]
29. Qian, L.; Xie, Y.; Zhang, S.; Zhang, J. Band Engineering of Carbon Nanotubes for Device Applications. *Matter* **2020**, *3*, 664–694. [CrossRef]
30. Chen, C.-W.; Lee, M.-H.; Clark, S. Band gap modification of single-walled carbon nanotube and boron nitride nanotube under a transverse electric field. *Nanotechnology* **2004**, *15*, 1837–1843. [CrossRef]
31. Liu, X.; Han, M.; Zhang, X.; Hou, H.; Pang, S.; Wu, Q. Tuning Electronic Structures of BN and C Double-Wall Hetero-Nanotubes. *J. Nanomater.* **2015**, *2015*, 326294. [CrossRef]
32. Akter, N.; Mawardi Ayob, M.T.; Radiman, S.; Khandaker, M.U.; Osman, H.; Alamri, S. Bio-Surfactant Assisted Aqueous Exfoliation of High-Quality Few-Layered Graphene. *Crystals* **2021**, *11*, 944. [CrossRef]
33. Yuan, Y.; Wang, F. A comparison of three DFT exchange-correlation functionals and two basis sets for the prediction of the conformation distribution of hydrated polyglycine. *J. Chem. Phys.* **2021**, *155*, 094104. [CrossRef] [PubMed]
34. Geiger, R.; Zabel, T.; Sigg, H. Group IV direct band gap photonics: Methods, challenges, and opportunities. *Front. Mater.* **2015**, *2*, 52. [CrossRef]
35. Crowley, J.M.; Tahir-Kheli, J., III. Resolution of the Band Gap Prediction Problem for Materials Design. *J. Phys.* **2016**, *7*, 1198–1203. [CrossRef] [PubMed]
36. Zviagin, V.; Grundmann, M.; Schmidt-Grund, R. Impact of Defects on Magnetic Properties of Spinel Zinc Ferrite Thin Films. *Phys. Status Solidi B* **2020**, *257*, 1900630. [CrossRef]
37. Wang, G. First-Principles Studies of Group IV and Group V Related Two Dimensional Materials. Ph.D. Thesis, Michigan Technological University, Houghton, MI, USA, 2016. [CrossRef]
38. Punter, A.; Nava, P.; Carissan, Y. Atomic pseudopotentials for reproducing π-orbital electron behavior in sp^2 carbon atoms. *Int. J. Quantum Chem.* **2019**, *119*, 25914. [CrossRef]
39. Li, R.; Cao, H.; Dong, J. Electronic properties of group-IV monochalcogenide nanoribbons: Studied from first-principles calculations. *Phys. Lett. A* **2017**, *381*, 3747–3753. [CrossRef]
40. Sun, Y.; Nishida, T. *Band Structures of Strained Semiconductors*; Springer: Boston, MA, USA, 2009. [CrossRef]
41. Landau, A.; Khistyaev, K.; Dolgikh, S.; Krylov, A.I. Frozen natural orbitals for ionized states within equation-of-motion coupled-cluster formalism. *J. Chem. Phys.* **2010**, *132*, 014109. [CrossRef]

42. Steeve, C.; Salahub, D.R. Density Functional Theory, Methods, Techniques, and Applications. In *Atomic Clusters and Nanoparticles. Agregats Atomiques et Nanoparticules*; Springer: Berlin/Heidelberg, Germany, 2000; Volume 73, pp. 105–160.
43. Cohen, A.J.; Mori-Sánchez, P.; Yang, W. Insights into Current Limitations of Density Functional Theory. *Science* **2008**, *321*, 792–794. [CrossRef]
44. Garza, J.; Vargas, R.; Nichols, J.; Dixon, D.A. Orbital energy analysis with respect to LDA and self-interaction corrected exchange-only potentials. *J. Chem. Phys.* **2001**, *114*, 639–651. [CrossRef]
45. Giarusso, S.; Gori-Giorgi, P. Exchange-Correlation Energy Densities and Response Potentials: Two Definitions and Analytical Model for the Strong-Coupling Limit of a Stretched Bond. *J. Phys. Chem.* **2020**, *124*, 2473–2482. [CrossRef]
46. Grüning, M.; Gritsenko, O.V.; Baerends, E.J. Exchange-correlation energy and potential as approximate functionals of occupied and virtual Kohn-Sham orbitals: Application to dissociating H_2. *J. Chem. Phys.* **2003**, *118*, 7183. [CrossRef]